Mon. Not. R. Astron. Soc. **348,** 250–260 (2004)

# Non-linear galaxy power spectrum and cosmological parameters

Asantha Cooray★
*Theoretical Astrophysics, Mail Code 130-33, Caltech, Pasadena, CA 91125, USA*

Accepted 2003 October 27. Received 2003 October 15; in original form 2003 August 12

**ABSTRACT**

The galaxy power spectrum is now a well-known tool of precision cosmology. In addition to the overall shape, baryon oscillations and the small-scale suppression of power by massive neutrinos capture complementary information on cosmological parameters when compared with the angular power spectrum of cosmic microwave background anisotropies. We study both the real-space and redshift-space galaxy power spectra in the context of non-linear effects, and model them based on the halo approach to large-scale structure clustering. We consider potential systematics in the cosmological parameter determination when non-linear effects are ignored and the galaxy power spectrum is described with the linear power spectrum scaled by a constant bias factor. We suggest that significant improvements can be made when non-linear effects are taken into account as a power-law contribution with two additional parameters to be determined from the data. In addition to cosmological parameters through galaxy clustering, such an approach allows a determination of useful information related to astrophysics on how galaxies occupy dark matter haloes.

**Key words:** galaxies: clusters: general – galaxies: distances and redshifts – cosmological parameters – cosmology: theory – dark matter – large-scale structure of Universe.

## 1 INTRODUCTION

Through a statistical measurement of information related to inhomogeneities in the Universe, the galaxy power spectrum provides a strong tool in the present era of precision cosmology. In addition to information related to the primordial power spectrum, characterized by a slope and a normalization, through a turnover at $k_{\rm eq} \equiv \sqrt{2\Omega_{\rm m}H_0^2(1+z_{\rm eq})}$, the overall shape of the galaxy power spectrum captures cosmological information related to the horizon at the matter–radiation equality. In addition to the overall shape, additional features in the galaxy power spectrum allow improved measurements of several cosmological parameters. Similar to the oscillatory features in the cosmic microwave background (CMB) anisotropy power spectrum, the matter power spectrum is expected to exhibit the presence of baryons through oscillations. These features are associated with the sound horizon at the end of the Compton-drag epoch and capture information related to $\Omega_{\rm m}h^2$ and $\Omega_{\rm b}h^2$ (Eisenstein & Hu 1998).

Unlike well-known oscillatory features in the angular power spectrum of CMB anisotropies, baryon-related oscillations in the matter power spectrum of the large-scale structure are highly suppressed due to the low baryon to dark matter ratio. For currently favoured $\Lambda$CDM cosmologies, baryon oscillations in the matter power spectrum have amplitude variations at the level of $\sim$8 per cent with effective widths in Fourier space of the order of $\Delta k \sim 0.03\,h\,{\rm Mpc}^{-1}$.

★E-mail: asante@caltech.edu

While the ideal way to detect baryon oscillations is to measure the three-dimensional dark matter power spectrum directly, unfortunately, there are no useful probes of this quantity. Effects such as weak gravitational lensing that trace matter fluctuations only provide information related to the projected power spectrum over a broad window function in redshift space (e.g. Bartelmann & Schneider 2001). This leads to an averaging of small features such as baryon oscillations such that they remain undetectable even considering the most favourable scenarios.

Galaxy redshift surveys, on the other hand, allow a measurement of the three-dimensional power spectrum of the galaxy distribution. Since galaxies are expected to trace matter fluctuations, at least in large and linear scales, the galaxy power spectrum has been pursued for an observational detection of baryon oscillations. When detected, baryon oscillations are expected to allow significant improvements in parameter determination by breaking various degeneracies associated with the interpretation of CMB data (Eisenstein, Hu & Tegmark 1998; Eisenstein 2002; Cooray 2002a; Blake & Glazebrook 2003). While expectations for precision parameter measurements are generally high, these have been tested to some extent with measured power spectra from redshift surveys such as the 2dF Galaxy Redshift Survey (2dFGRS; Colless et al. 2001) when combined with recent results from CMB anisotropy experiments (e.g. Percival et al. 2002). The same surveys have allowed first attempts to detect baryon oscillations, though there is still no significant evidence for them (e.g. Percival et al. 2001; see also Miller, Nichol & Batuski 2001). This can be understood by the fact that three-dimensional redshift surveys, so far, lack the required volume, with sizes of the

order of $L \sim 2\,\pi/\Delta k \sim 300\,h^{-1}$ Mpc in each dimension, to resolve them reliably.

In addition to galaxy redshift surveys, a number of additional observational efforts are either under way or planned to image the large-scale structure out to a redshift of a few. These wide-field surveys typically cover tens to thousands of square degrees on the sky and include weak gravitational lensing shear observations with instruments such as the *Supernova Acceleration Probe* (*SNAP*; Massey et al. 2003) and the Large Aperture Synoptic Survey Telescope (LSST; Tyson, Wittman & Angel 2000), and observations of the Sunyaev–Zel'dovich (SZ) effect Sunyaev & Zel'dovich (1980) with dedicated small angular scale CMB telescopes such as the South Pole Telescope (SPT; Stark et al. 1998). These surveys are expected to produce catalogues of dark matter haloes, which in the case of lensing and SZ surveys are expected to be essentially mass-selected (Holder et al. 2000; Wittman et al. 2001). While the halo number count as a function of redshift is a well-known cosmological test (Haiman, Mohr & Holder 2001), one can also consider the additional information supplied by the clustering of haloes. In particular, similar to the approach in galaxy redshift surveys, one can measure the power spectrum of clustering associated with these haloes, as a whole, and use that power spectrum for cosmological studies. In addition to the shape, cosmological information comes from the redshift evolution of *rulers* that can be calibrated through CMB data (Cooray et al. 2001; Blake & Glazebrook 2003).

The cosmological studies based on the galaxy power spectrum and related halo clustering information, unfortunately, is affected by non-linearities. While sources are expected to trace inhomogeneities in mass due to the non-linear evolution of gravitational perturbations at late times, the galaxy power spectrum at small scales departs significantly from the linear description corrected for source bias. The enhancement of power due to non-linearities erases oscillatory features (Meiksin, White & Peacock 1996), while effects such as redshift-space distortions further contribute to their disappearance. Owing to the cosmological significance of baryon oscillations, suggestions have already been made to detect them at redshifts of a few since the non-linear scale at high redshift is expected to move to smaller scales than today (Eisenstein 2002; Blake & Glazebrook 2003).

In the case of current measurements, the cosmological interpretation is restricted only for large scales where clustering is expected to be linear. The standard approach to describe the galaxy power spectrum involves the linear power spectrum scaled by a constant bias factor (e.g. Percival et al. 2001). While slight modifications to the bias description have been considered (Elgaroy & Lahav 2003), there is still no guidance as to how non-linearities affect cosmological parameter measurements and what approaches can be made to improve such estimates. Additionally, by restricting cosmological interpretation to specific range of wavenumbers, it is likely that we have only extracted limited information from current data. For example, in the case of the 2dFGRS, analyses have only been considered out to a wavenumber of $0.15\,h\,\mathrm{Mpc}^{-1}$, while measurements span to considerably smaller scales. It is clear that further studies are needed on galaxy clustering well into the non-linear regime, and to understand what information can be extracted from the non-linear regime of clustering or, at least, from the transition regime where non-linearities become important.

The purpose of this paper is to understand the onset of non-linearities in the galaxy power spectrum. While detailed numerical simulations are useful for this purpose, here we make use of the halo approach to galaxy clustering (Seljak 2000; Peacock & Smith 2000; Scoccimarro et al. 2001; Sheth & Diaferio 2001; Berlind & Weinberg 2002). The halo approach provides a useful tool to understand certain aspects of clustering and is a physically consistent model without any prior assumptions on the biasing nature of galaxies with respect to the dark matter distribution (for a review, see Cooray & Sheth 2002). We study how cosmological parameter measurements can be improved by extracting information from mildly non-linear scales that are currently ignored. In particular, we pay attention to systematics that are introduced to cosmological parameter measurements when the galaxy power spectrum is modelled simply with a scaled version of the linear power spectrum. We show that parameter estimates are biased away from the true values and that these departures can be significantly reduced when the non-linear contribution, at least near the regime of transition from linear to non-linear clustering, is modelled as a power law. Since parameters related to this description are determined from data simultaneously with cosmological parameter estimates, this approach leads to a slight degradation of errors associated with cosmological parameters alone. The main advantage is that these estimates, however, remain either unbiased or biased at a level that is negligible. The suggested approach can be easily implemented with current studies and when interpreting results related to completed 2dFGRS and SDSS surveys (York et al. 2000), among others. The suggested approach also avoids an arbitrary distinction as to what scales correspond to the linear regime of clustering while also allowing the maximum extraction of cosmological information from data.

The paper is organized as follows. In the next section, we outline the main considerations related to the halo approach to galaxy clustering. We refer the reader to the review by Cooray & Sheth (2002) for full details of this approach. We make use of the Fisher matrix approach to quantify biases and expected errors on parameter measurements in Section 3. In Section 4, we conclude with a summary.

## 2 HALO APPROACH TO CLUSTERING

### 2.1 Real-space clustering

The halo approach provides a physically motivated scheme to understand non-linear clustering of dark matter and various tracer populations of the large-scale structure (see Cooray & Sheth 2002, for more details). Under this description, the galaxy spectrum takes the form of

$$P_{\rm gal}(k) = P^{\rm 1h}_{\rm gal}(k) + P^{\rm 2h}_{\rm gal}(k), \tag{1}$$

where

$$P^{\rm 1h}_{\rm gal}(k) = \int {\rm d}m\; n(m) \frac{\langle N_{\rm gal}(N_{\rm gal}-1)\,|\,m\rangle}{\bar{n}^2_{\rm gal}} |u_{\rm gal}(k\,|\,m)|^p,$$

$$P^{\rm 2h}_{\rm gal}(k) = P^{\rm lin}(k) \left[\int {\rm d}m n(m) b_1(m) \frac{\langle N_{\rm gal}\,|\,m\rangle}{\bar{n}_{\rm gal}} u_{\rm gal}(k\,|\,m)\right]^2.$$

Here,

$$\bar{n}_{\rm gal} = \int {\rm d}m n(m) \langle N_{\rm gal}\,|\,m\rangle \tag{2}$$

denotes the mean number density of galaxies and

$$u_{\rm gal}(k\,|\,m) = \int_0^{r_{\rm vir}} {\rm d}r 4\pi r^2 \frac{\sin kr}{kr} \frac{\rho_{\rm gal}(r\,|\,m)}{m} \tag{3}$$

denotes the normalized Fourier transform of the galaxy density distribution within a halo of mass $m$. The standard assumption here is

that galaxies trace dark matter within haloes such that one can utilize the dark matter distribution given by analytic forms such as the NFW (Navarro, Frenk & White 1996) profile. An improved approximation will be to use the density distribution defined by subhaloes. Since relevant profiles related to substructure are still not well studied numerically, we make use of the dark matter density profile to describe the galaxy distribution within haloes. In equations (1) and (2), $n(m)$ is the halo mass function (e.g. Press & Schechter 1974) and $b_1(m)$ is the halo bias relative to linear clustering (Mo & White 1996).

An important ingredient in the halo description of galaxy clustering is the halo occupation number (Kauffmann et al. 1999; Benson et al. 2000; Berlind et al. 2003). Following Sheth & Diaferio (2001), for the illustration of non-linear effects related to galaxy clustering, we take a description motivated by semi-analytic models:

$$\langle N_{\rm gal} \,|\, m\rangle = \begin{cases} N_0 & \text{for } 10^{11}\ {\rm M}_\odot\ h^{-1} \leqslant m \leqslant M_{\rm B}, \\ N_0 (m/M_{\rm B})^{\alpha} & \text{for } m > M_{\rm B}, \end{cases} \tag{4}$$

where we set $M_{\rm B} = 4 \times 10^{12}\ {\rm M}_\odot/h$ and take $\alpha$ and $N_0$ as free parameters. In our fiducial description, these two parameters take numerical values of 0.8 and 0.7, respectively.

In addition to the mean number of galaxies as a function of halo mass, for the one-halo term of the power spectrum (equation 1), we need information related to the second moment of the halo occupation number, $\langle N_{\rm gal}(N_{\rm gal}-1) \,|\, m\rangle$. If the probability distribution function for galaxy occupation is Poisson, then $\langle N_{\rm gal}(N_{\rm gal}-1) \,|\, m\rangle = \langle N_{\rm gal} \,|\, m\rangle^2$, though departures from the Poisson description are clearly visible in numerical data (Berlind et al. 2003). Following Scoccimarro et al. (2001), we make use of the binomial distribution, matched to numerical data, to obtain a convenient approximation. The second moment is then

$$\langle N_{\rm gal}(N_{\rm gal}-1)\rangle^{1/2} = \beta(m) \langle N_{\rm gal} \,|\, m\rangle, \tag{5}$$

where $\beta(m) = \log\sqrt{m/10^{11}\ h^{-1}\ {\rm M}_\odot}$ for $m < 10^{13}\ h^{-1}\ {\rm M}_\odot$ and $\beta(m) = 1$ thereafter. Note that in equation (1), the simplest approach is to set $p = 2$ when calculating $P^{\rm 1h}_{\rm dm}(k)$. In haloes that contain only a single galaxy, however, it is natural to assume that this galaxy sits at the centre. Thus, an improved model for the galaxy distribution is to take $p = 2$ when $\langle N_{\rm gal}(N_{\rm gal}-1)\rangle$ is greater than unity and $p = 1$ otherwise.

In Fig. 1, we show the galaxy power spectrum calculated following the halo model and a comparison to the non-linear dark matter power spectrum, again calculated under the halo model; to describe dark matter clustering, one removes information related to the halo occupation number and the number density of galaxies from equation (1). Note that, in Fig. 1 and throughout, we plot the logarithmic power spectrum, $\Delta^2(k) \equiv k^3 P(k)/2\pi^2$ instead of $P(k)$ itself. We also show a measurement of the real-space power spectrum from the *IRAS* PSCZ survey (Saunders et al. 1990) as determined by Hamilton & Tegmark (2002). In the bottom plot of Fig. 1, we show the transition regime between linear and non-linear clustering. At large scales, where the two-halo term dominates, the galaxy power spectrum traces the linear clustering with a constant bias. One can understand this by noting that, at large scales, $u_{\rm gal}(k \,|\, m) \to 1$ and the galaxy power spectrum simplifies to

$$P_{\rm gal}(k) \approx b^2_{\rm gal} P^{\rm lin}(k), \tag{6}$$

with

$$b_{\rm gal} = \int {\rm d}m\ n(m)\ b_1(m) \frac{\langle N_{\rm gal} \,|\, m\rangle}{\bar{n}_{\rm gal}} \tag{7}$$

denoting the mean bias factor of the galaxy population.

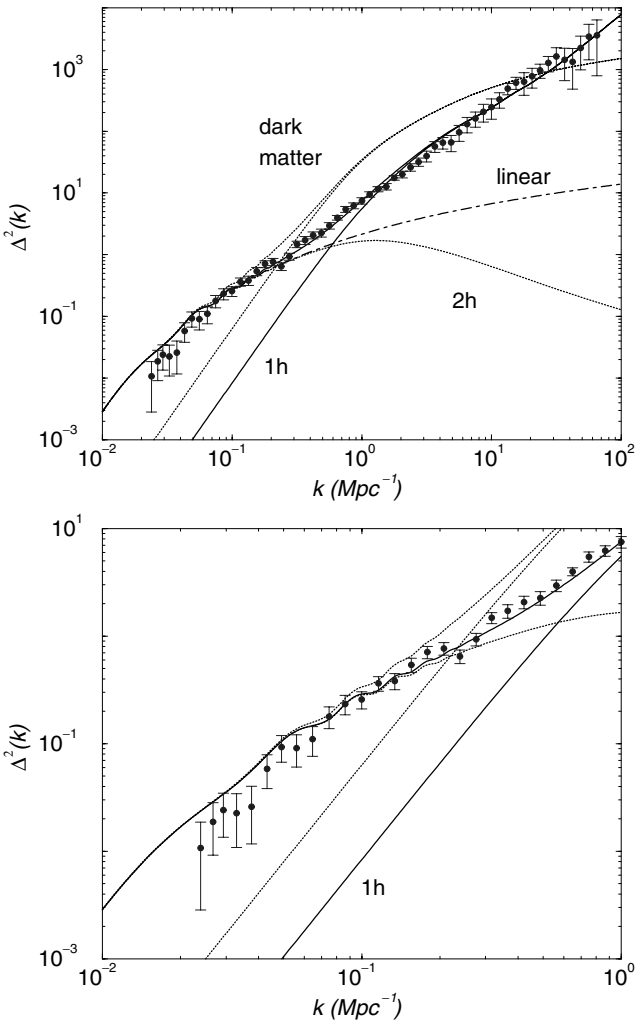


**Figure 1.** The galaxy power spectrum in real space (solid lines) and a comparison to the clustering in dark matter (dotted lines). We show the one- and two-halo contributions to the galaxy power spectrum and the one-halo contribution to the dark matter power spectrum. For reference, the dot-dashed line shows the linear power spectrum. The measured data points represent the power spectrum of the *IRAS* Point Source Catalog Redshift Survey (PCSz; Saunders et al. 1990) as measured by Hamilton & Tegmark (2002). In the bottom panel, we consider the transition regime between linear and non-linear clustering. As we discuss later, the transition to non-linear clustering can be described via a combination of the linear power spectrum scaled with a constant, scale-free, bias and an additional contribution that is a power law.

This is consistent with the standard assumption in the literature that the galaxy bias, at large scales, is constant. The drawback with this description is that the physical scale below which this assumption breaks down is ill defined. It is generally assumed that the onset of non-linearity is at wavenumbers $\sim 0.1\ h\ {\rm Mpc}^{-1}$, though this is only based on numerical simulations of the non-linear dark matter power spectrum. While such a scale is valid for the dark matter distribution, when considering galaxies there is no reason why the same situation should hold. In the case of the halo approach to galaxy clustering, the onset of non-linearities, by which we assume the dominance of the one-halo term, is model-dependent. To illustrate this, in Fig. 2, we model the galaxy power spectrum as a function of $\alpha$ and $N_0$. Note that the transition is strongly sensitive to $\alpha$ such that, when $\alpha$ is low, the galaxy power spectrum traces the

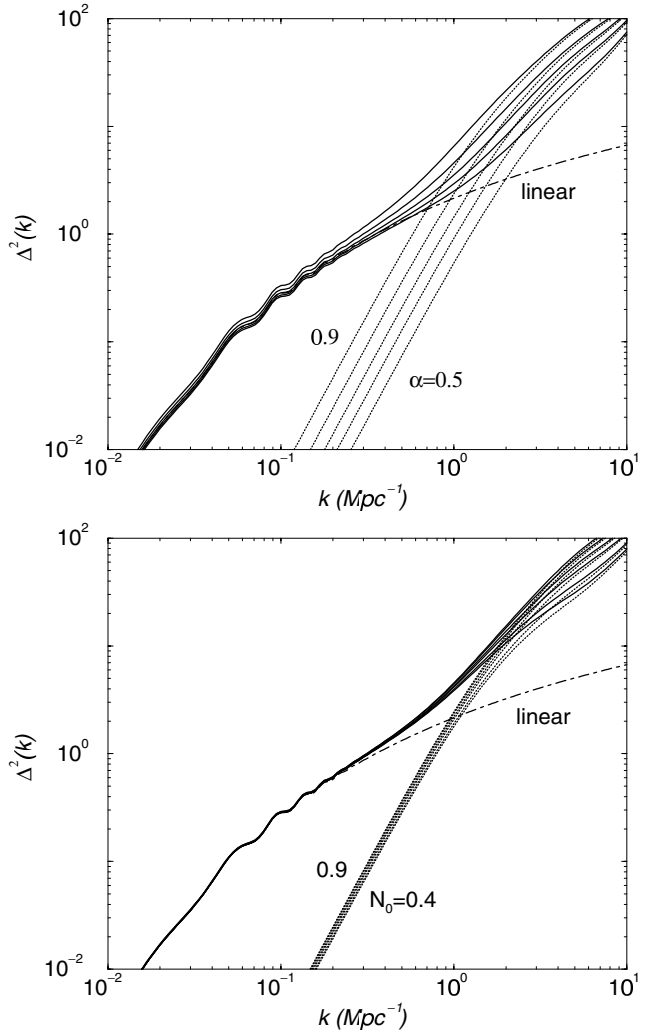


**Figure 2.** The dependence of the real-space galaxy power spectrum on model parameters related to the halo occupation number. In the top panel we show variations related to $\alpha$ (with $N_0 = 0.7$), and in the bottom panel variations related to $N_0$ (with $\alpha = 0.8$). As shown, the slope of the mean number of galaxies as a function of halo mass strongly determines the scale at which the one-halo term, the non-linear contribution, dominates the total power spectrum.

linear clustering down to relatively smaller scales, $\sim$0.5 Mpc$^{-1}$, while when $\alpha$ is high (>0.8), the onset of non-linearity is near 0.1 Mpc$^{-1}$. If $\langle N_{\rm gal} \mid m\rangle$ simply scales as $N_0(m/M_{\rm B})^{\alpha}$, then the galaxy power spectrum is independent of $N_0$, as one renormalizes by the galaxy number density, which is also an integral of this quantity weighted by the mass function. In Fig. 2, we see slight dependences on $N_0$ since the halo occupation number was modelled with two parts, one that is a constant and another involving a power law. In this case, the one-halo term is slightly dependent on the numerical value of $N_0$.

### 2.2 From real space to redshift space

So far, we have only considered the real-space power spectrum of galaxies. Observationally, for example in the case of the 2dF survey, the galaxy power spectrum is measured from redshift surveys, and additional corrections must be taken into account when modelling clustering in redshift space. Following Kaiser (1987), we can write the redshift-space fluctuation, $\delta_{\rm g}^z$, of galaxy density field, relative to the real-space fluctuation, $\delta_{\rm g}$, as

$$\delta_{\rm g}^z(\boldsymbol{k}) = \delta_{\rm g}(\boldsymbol{k}) + \delta_{\rm v}\mu^2, \tag{8}$$

where $\delta_{\rm v}$ is the divergence of the velocity field and $\mu = \hat{\boldsymbol{r}} \cdot \hat{\boldsymbol{k}}$ is the line-of-sight angle. At linear scales, one can simplify the relation by noting that $\delta_{\rm g}(\boldsymbol{k}) = b_{\rm g}\delta(\boldsymbol{k})$ and $\delta_{\rm v} = f(\Omega_{\rm m})\delta(\boldsymbol{k})$ with $f(\Omega_{\rm m}) = {\rm d}\log\delta/{\rm d}\log\, a \approx \Omega_{\rm m}^{0.6}$ to obtain

$$\delta_{\rm g}^z(\boldsymbol{k}) = \delta_{\rm g}(\boldsymbol{k})(1 + \beta\mu^2), \tag{9}$$

where $\beta = f(\Omega_{\rm m})/b_{\rm g}$. The latter is generally measured from redshift surveys since it allows a determination of $\Omega_{\rm m}$ through constraints on the bias factor (Strauss & Willick 1995; Outram et al. 2001; Peacock et al. 2001). At linear scales, the distortions increase power by a factor of $(1 + \frac{2}{3}\beta + \frac{1}{5}\beta^2)$, which when $b_{\rm g} = 1$ is 1.41 for $\Omega_{\rm m} = 0.35$. At non-linear scales, virial velocities within haloes modify clustering properties. With a Gaussian description for one-dimensional virial motions, we write

$$\delta_{\rm g}^z(\boldsymbol{k}) = \delta_{\rm g}\, {\rm e}^{-(k\sigma\mu)^2/2}. \tag{10}$$

Putting all terms together, under the halo approach, we can write the power spectrum in redshift space as (Seljak 2001)

$$P_{z,{\rm gal}}(k) = P_{z,{\rm gal}}^{1\,{\rm h}}(k) + P_{z,{\rm gal}}^{2\,{\rm h}}(k), \tag{11}$$

where

$$P_{z,{\rm gal}}^{1\,{\rm h}}(k) = \int {\rm d}m\; n(m) \frac{\langle N_{\rm gal}(N_{\rm gal}-1) \mid m\rangle}{\bar{n}_{\rm gal}^2} R_p(k\sigma)|u_{\rm gal}(k \mid m)|^p,$$
$$P_{z,{\rm gal}}^{2\,{\rm h}}(k) = \left(F_{\rm g}^2 + \tfrac{2}{3}F_{\rm v}F_{\rm g} + \tfrac{1}{5}F_{\rm v}^2\right) P^{\rm lin}(k),$$

with

$$F_{\rm g} = \int {\rm d}m\; n(m)\; b_1(m) \frac{\langle N_{\rm gal} \mid m\rangle}{\bar{n}_{\rm gal}} R_1(k\sigma) u_{\rm gal}(k \mid m),$$
$$F_{\rm v} = f(\Omega_{\rm m}) \int {\rm d}m\; n(m)\; b_1(m)\; R_1(k\sigma) u(k \mid m), \tag{12}$$

and

$$R_p(\alpha = k\sigma\sqrt{p/2}) = \frac{\sqrt{\pi}}{2}\frac{{\rm erf}(\alpha)}{\alpha}, \tag{13}$$

for $p = 1, 2$. In equation (11), $\bar{n}_{\rm gal}$ denotes the mean number density of galaxies (equation 2).

In order to model velocities within virialized haloes, we make use of a description based on isothermal spheres and in reasonable agreement with measurements of virial velocities within haloes in numerical simulations (Sheth & Diaferio 2001). If $\sigma_{\rm vir}$ denotes the one-dimensional velocity dispersion of particles within a halo, then

$$\sigma_{\rm vir} = \gamma \left(\frac{Gm}{2r_{\rm vir}}\right)^{0.5}, \tag{14}$$

where the virial radius is related to the halo mass through $M_{\rm vir} = 4\pi\Delta\bar{\rho}r_{\rm vir}^3/3$ and $\gamma$ is a free parameter that we use here to demonstrate how uncertainties related to virial motion affect the predicted non-linear contribution to the redshift-space power spectrum of galaxies.

Even though peculiar velocities increase power at large scales, virial motions within haloes lead to a suppression of power. In Fig. 3, we show the power spectra of dark matter and galaxies in redshift space with a comparison to that of real space. While clustering power is increased at large scales, for both dark matter and galaxies, the power is reduced substantially at scales where the one-halo term of the power spectrum dominates. This is easily understandable since

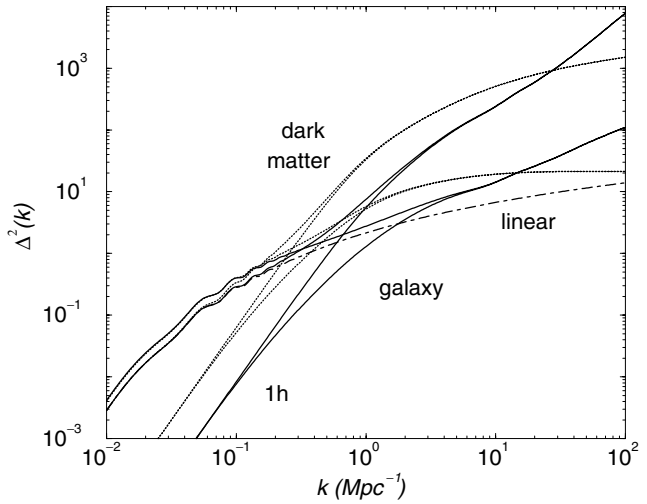


**Figure 3.** The power spectrum of dark matter (dotted lines) and galaxies (solid lines) in redshift space. For comparison, we also show the real-space power spectrum, which is lower than the redshift-space spectrum at large scales and higher at non-linear scales. The increase in power at large scales is associated with bulk motions of haloes, while virial motions within haloes lead to a suppression of power associated with the one-halo term of the halo description.

the virial motions within haloes lead to a decrease in power when averaged over all angles.

As a comparison to observable data so far, to model the 2dFGRS redshift-space power spectrum, we move from theory space description to the observable space by convolving the theory power spectrum over the 2dF survey window function:

$$W^2_{\rm 2dF}(k) = \frac{1}{1+(k/a)^2+(k/b)^4}, \tag{15}$$

where $a = 0.003\,42$ and $b = 0.009\,83$ (Elgaroy, Gramann & Lahav 2002). The observed power spectrum is then given by

$$P_{\rm 2dF}(k) = \int {\rm d}^3\boldsymbol{k}' P_{z,{\rm gal}}(|\boldsymbol{k}-\boldsymbol{k}'|)\widehat{W}^2_{\rm 2dF}(k'), \tag{16}$$

where $\widehat{W}$ is the normalized window function such that $\int {\rm d}^3k \widehat{W}^2_{\rm 2dF}(k) = 1$.

In Fig. 4, we show predicted redshift-space galaxy power spectra convolved with the 2dF window function. As a comparison, we also plot the 2dFGRS power spectrum from Percival et al. (2001). Note that we have not attempted to model the 2dF data by varying parameters of either the cosmological model or the halo description, but rather we show data to guide in understanding how non-linearities can affect current interpretations of the 2dF power spectrum. A model fit to halo occupation number, based on the 2dF correlation function, can be found in Magliocchetti & Porciani (2003). In the middle and bottom panels of Fig. 4, we show the convolved redshift-space power spectrum as a function of parameters in the halo description, mainly mass slope of the halo occupation number and the normalization of the virial equation that determines galaxy motions within haloes. For comparison, we also show the linear prediction, again convolved with the 2dF window function. One should note the lack of oscillatory features in these power spectra when compared with those in Fig. 3. This is due to the averaging over the 2dF window function and leads to a reduction in amplitude of small-scale features (e.g. Elgaroy et al. 2002).

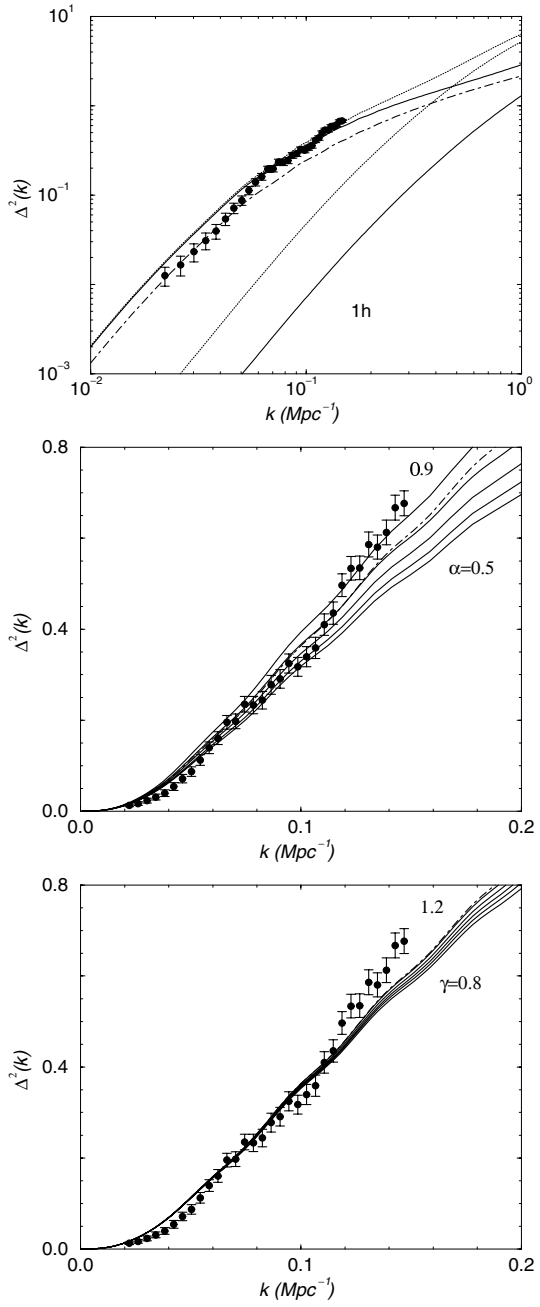


**Figure 4.** The redshift-space power spectrum of the 2dFGRS (data points from Percival et al. 2001). The solid lines show the redshift-space galaxy power spectrum convolved with the 2dF window function. Note the lack of baryon oscillation features due to smearing of modes over the finite width of the filter. For comparison, we also show the linear (dot-dashed line) and the redshift-space dark matter (dotted lines) power spectra, again convolved with the 2dF window function. The middle and bottom panels are variations on the predicted redshift-space galaxy power spectrum as a function of $\alpha$, the mass slope of the halo occupation number, and $\gamma$, the normalization of the virial equation. In the middle panel, we assume $\gamma = 1$, while the bottom panel fixes $\alpha$ to be 0.8. In both cases, $N_0$ is taken to be 0.7.

As shown in Fig. 4, the redshift-space galaxy power spectrum is such that the transition to non-linearity comes with a reduction of power, relative to the scaled linear power spectrum with a constant bias. This is opposite to the case associated with the real-space power spectrum, where the onset of non-linearity is always

associated with an increase in power relative to the linear power spectrum scaled by a constant bias. Another way to state this observation is that the bias factor for galaxies in redshift space, relative to linear clustering, decreases from a constant value at large scales when non-linearities become important. As one moves to much smaller scales ($k > 10$ Mpc$^{-1}$), the non-linear redshift space power spectrum dominates over the linear description and the bias factor increases back to a higher value (see Fig. 3). This is consistent with calculations of the redshift-space bias by Seljak (2000). As shown in Fig. 4, we found the reduction in non-linear power to be present when certain parameters related to the halo model description is varied and we consider this to be a general feature of the redshift-space power spectrum.

In general, our calculations indicate that the linear assumption is only valid out to $\sim$0.1 Mpc$^{-1}$ in the case of both the real- and the redshift-space power spectra, and proper modelling of these data beyond such a scale must include some accounting for non-linearities. If measurements beyond 0.1 Mpc$^{-1}$ are used for cosmological purposes, with a constant bias factor, one can potentially misidentify the drop in power due to non-linearities as due to a cosmological effect, for example, due to a massive neutrino since massive neutrinos are expected to damp power at small scales. In the next section, we address this issue in detail using the Fisher matrix based approach to quantify how non-linearities affect cosmological parameter determination and what improvements can be introduced to avoid potential biases.

## 3 NON-LINEARITIES AND COSMOLOGY

To quantify the extent to which cosmological parameters can be affected by assumptions in the literature and to calculate expected errors on cosmological parameters and associated biases, we make use of the Fisher information matrix:

$$\boldsymbol{F}_{ij} = -\left\langle \frac{\partial^2 \ln L}{\partial p_i \partial p_j} \right\rangle_{\boldsymbol{x}}, \tag{17}$$

whose inverse provides the optimistic covariance matrix for errors on the associated parameters (e.g. Tegmark, Taylor & Heavens 1997). In equation (17), $L$ is the likelihood of observing data set $\boldsymbol{x}$, in our case the power spectrum, given the parameters $p_1, \ldots, p_n$ that describe these data. Following the Cramér–Rao inequality (Kendall & Stuart 1969), no unbiased method can measure the $i$th parameter with standard deviation less than $(\boldsymbol{F}_{ii})^{-1/2}$ if all other parameters are exactly known, and less than $[(\boldsymbol{F}^{-1})_{ii}]^{1/2}$, from the inverse of the Fisher matrix, if other parameters are to be estimated from the data as well.

For this discussion, we first focus on the binned real-space galaxy power spectrum and return to the case involving the redshift-space power spectrum as part of the discussion. The binned power spectrum can be written as an integral average over a shell in $k$-space centred around some wavenumber $k_i$ with width $\Delta k$:

$$\hat{P}_i = \frac{1}{V}\int_i \frac{\mathrm{d}^3k}{V_i} P(k), \tag{18}$$

where $V_i = 4\pi\, k_i^2 \Delta k$ is the shell volume and $V$ is the total survey volume. The full covariance related to measurement of this binned power spectrum is (Scoccimarro, Zaldarriaga & Hui 1999; Meiksin & White 1999; Cooray & Hu 2001)

$$\begin{aligned}\mathcal{C}_{ij} &= \langle \hat{P}_i \hat{P}_j \rangle - \langle \hat{P}_i \rangle \langle \hat{P}_j \rangle \\ &= \frac{1}{V}\left[\frac{(2\pi)^3}{V_i} 2\hat{P}_i'^2 \delta_{ij} + T_{ij}\right],\end{aligned} \tag{19}$$

where

$$T_{ij} = \int_i \frac{\mathrm{d}^3k}{V_i}\int_j \frac{\mathrm{d}^3k}{V_j} T(\boldsymbol{k}_i, -\boldsymbol{k}_i, \boldsymbol{k}_j, -\boldsymbol{k}_j) \tag{20}$$

is the non-Gaussian contribution to the covariance of the power spectrum. This non-Gaussian contribution depends on parallelogram configurations of the trispectrum, $T(\boldsymbol{k}_i, -\boldsymbol{k}_i, \boldsymbol{k}_j, -\boldsymbol{k}_j)$, and we make use of the one-halo term of the halo approach (Cooray & Sheth 2002) to calculate it following Cooray & Hu (2001). This approach is a valid description since in linear scales the covariance is dominated by the Gaussian variance while non-Gaussianities are only significant in non-linear scales where the one-halo term dominates. We can write the relevant contribution as

$$\begin{aligned}T_{ij} = &\int_i \frac{\mathrm{d}^3k}{V_i}\int_j \frac{\mathrm{d}^3k}{V_j}\int \mathrm{d}m\; n(m) \\ &\times \frac{\langle N_{\rm gal}\cdots(N_{\rm gal}-3)\,|\,m\rangle}{\bar{n}_{\rm gal}^4} |u_{\rm gal}(k_i\,|\,m)|^2 |u_{\rm gal}(k_j\,|\,m)|^2,\end{aligned} \tag{21}$$

where $\langle N_{\rm gal}(N_{\rm gal}-3)\,|\,m\rangle$ is the fourth moment of the halo occupation distribution. We follow our previous description related to the galaxy power spectrum and write

$$\langle N_{\rm gal}\cdots(N_{\rm gal}-3)\,|\,m\rangle = \beta^2(m)[2\beta^2(m)-1][3\beta^2(m)-2]\langle N_{\rm gal}\rangle^4,$$

where departures from the Poisson model, denoted with the function $\beta(m)$ in equation (5), are related to the adopted binomial distribution following Scoccimarro et al. (2001). In equation (19), we allow for the shot-noise contribution to the power spectrum variance by redefining $\hat{P}_i' \rightarrow P_i + P^{\rm SN}$ such that the power spectrum is averaged over the shell with the shot-noise contribution of $P^{\rm SN} = 1/\bar{n}_{\rm g}$, where $\bar{n}_{\rm g} = N_{\rm g}/V$ is the number density of galaxies in the survey. In the Gaussian limit, the covariance only results in a diagonal error matrix with no correlations between band powers. This variance is given by the well-known formula (Peacock & West 1992; Blake & Glazebrook 2003)

$$\sigma^2(k) = 2\frac{(2\pi)^3}{V}\frac{1}{4\pi k^2 \Delta k}\left[P_{\rm gal}(k) + \frac{1}{\bar{n}_{\rm g}}\right]. \tag{22}$$

Using the full covariance, the Fisher matrix for the galaxy power spectrum can be written as (Cooray & Hu 2001)

$$\boldsymbol{F}_{\alpha\beta} = \sum_{ij}\frac{\partial \hat{P}_i}{\partial p_\alpha}[\mathcal{C}_{ij}]^{-1}\frac{\partial \hat{P}_j}{\partial p_\beta}, \tag{23}$$

where, for example, $p_\alpha$ denotes a cosmological parameter of interest. In addition to parameter errors, the Fisher matrix approach also allows a useful technique to quantify the biases associated with parameter estimates when the model description departs from the observations. For example, in the present case, the galaxy power spectrum is usually modelled with a combination of the linear power spectrum and a scale-free bias out to a certain wavenumber, beyond which no information is used for cosmological purposes. We can quantify the extent to which this is valid by studying parameter biases such that if $p_\alpha = \bar{p}_\alpha + \delta p_\alpha$, where $\bar{p}_\alpha$ is the true value of the parameter $\alpha$ and $\Delta p_\alpha$ is the resulting bias due to the wrong description of the power spectrum (in this case, linear power spectrum times constant bias), then

$$\delta p_\alpha = \sum_\beta F^{-1}_{\alpha\beta}\sum_{ij}[\bar{P}_i - \hat{P}_i][\mathcal{C}_{ij}]^{-1}\frac{\partial \hat{P}_j}{\partial p_\beta}, \tag{24}$$

where $\hat{P}_i$ and $\bar{P}_i(k)$ represent the true and erroneous binned galaxy power spectra at wavenumber $k_i$, respectively (e.g. Huterer 2002).

**Table 1.** Marginalized errors.[a] The top, central and bottom parts represent the parameter errors from galaxy clustering, galaxy clustering with the full three-year *WMAP* data, and galaxy clustering with *Planck* data.

| | $k < 0.1$ Mpc$^{-1}$ | | | $k < 0.2$ Mpc$^{-1}$ | | | $k < 0.5$ Mpc$^{-1}$ | | |
|---|---|---|---|---|---|---|---|---|---|
| Parameter | Error | Bias | \|Bias\|/Error | Error | Bias | \|Bias\|/Error | Error | Bias | \|Bias\|/Error |
| $\ln(\Omega_{\rm b}h^2)$ | 1.35 | 0.15 | 0.11 | 0.22 | 0.15 | 0.73 | 0.20 | 0.29 | 1.44 |
| $\ln(\Omega_{\rm m}h^2)$ | 1.29 | 0.06 | 0.05 | 0.31 | 0.05 | 0.17 | 0.29 | 0.08 | 1.75 |
| $m_\nu$ (eV) $\propto \Omega_\nu h^2$ | 5.64 | −1.01 | 0.18 | 1.59 | −1.90 | 1.19 | 1.35 | −7.54 | 5.56 |
| $\Omega_\Lambda$ | $\infty$ | – | – | $\infty$ | – | – | $\infty$ | – | – |
| $w$ | $\infty$ | – | – | $\infty$ | – | – | $\infty$ | – | – |
| $n_S(k_{\rm fid})$ | 0.58 | −0.04 | 0.06 | 0.09 | −0.22 | 2.34 | 0.08 | −0.66 | 8.74 |
| $\ln P_\Phi(k_{\rm fid}) \equiv \ln A_S^2$ | $\infty$ | – | – | $\infty$ | – | – | $\infty$ | – | – |
| $\ln b$ | $\infty$ | – | – | $\infty$ | – | – | $\infty$ | – | – |
| $\ln(\Omega_{\rm b}h^2)$ | 0.03 | 0.00 | 0.01 | 0.02 | 0.02 | 0.76 | 0.02 | 0.23 | 10.56 |
| $\ln(\Omega_{\rm m}h^2)$ | 0.06 | 0.00 | 0.03 | 0.05 | 0.06 | 1.25 | 0.04 | 0.39 | 8.38 |
| $m_\nu$ (eV) $\propto \Omega_\nu h^2$ | 0.38 | 0.06 | 0.09 | 0.23 | 0.94 | 4.23 | 0.21 | 3.48 | 16.77 |
| $\Omega_\Lambda$ | 0.07 | 0.00 | 0.00 | 0.06 | 0.02 | 0.33 | 0.06 | 0.16 | 2.92 |
| $w$ | 0.29 | −0.00 | 0.03 | 0.27 | −0.3 | 1.11 | 0.26 | −2.04 | 7.85 |
| $n_S(k_{\rm fid})$ | 0.018 | −0.00 | 0.04 | 0.015 | −0.03 | 2.02 | 0.01 | −0.24 | 18.67 |
| $\ln P_\Phi(k_{\rm fid}) \equiv \ln A_S^2$ | 0.021 | 0.00 | 0.00 | 0.017 | 0.02 | 1.07 | 0.016 | 0.19 | 12.00 |
| $\ln b$ | 0.040 | 0.00 | 0.09 | 0.034 | 0.06 | 1.93 | 0.033 | 0.06 | 1.77 |
| $\ln(\Omega_{\rm b}h^2)$ | 0.005 | 0.00 | 0.03 | 0.005 | 0.01 | 1.17 | 0.005 | 0.04 | 6.88 |
| $\ln(\Omega_{\rm m}h^2)$ | 0.015 | 0.01 | 0.06 | 0.013 | 0.04 | 2.84 | 0.012 | 0.20 | 16.21 |
| $m_\nu$ (eV) $\propto \Omega_\nu h^2$ | 0.17 | 0.02 | 0.10 | 0.12 | 0.72 | 5.78 | 0.09 | 3.47 | 38.43 |
| $\Omega_\Lambda$ | 0.05 | 0.00 | 0.00 | 0.049 | 0.00 | 0.03 | 0.05 | 0.022 | 0.44 |
| $w$ | 0.15 | −0.00 | 0.03 | 0.17 | −0.15 | 0.89 | 0.17 | −0.68 | 4.01 |
| $n_S(k_{\rm fid})$ | 0.004 | −0.00 | 0.04 | 0.004 | −0.01 | 2.43 | 0.003 | −0.05 | 16.95 |
| $\ln P_\Phi(k_{\rm fid}) \equiv \ln A_S^2$ | 0.005 | 0.00 | 0.01 | 0.005 | 0.01 | 1.03 | 0.004 | 0.04 | 8.92 |
| $\ln b$ | 0.017 | 0.00 | 0.06 | 0.016 | 0.05 | 2.92 | 0.013 | 0.36 | 26.91 |

[a]Parameter error calculation assumes following fiducial model: $\Omega_{\rm m} = 0.3$, $\Omega_{\rm b} = 0.04$, $\Omega_\Lambda = 0.7$, $h = 0.72$, $w = -1$ and $\Omega_\nu = 0$. We fix other parameters of interest related to CMB, $\tau = 0.1$ and $T/S = 0$, and assume a flat cosmology with $\Omega_{\rm K} = 0$. We quote $1\sigma$ errors. A parameter error of infinity implies that the parameter affects observables but is not constrained due to degeneracies; in particular, the normalization and bias are all degenerate and only broken through the addition of CMB data.

To calculate errors, we assume a galaxy redshift survey consistent with the SDSS and take $V_{\rm SDSS} = 10^8\ h^{-3}$ Mpc$^3$ and $N_{\rm g} = 5 \times 10^5$ such that the galaxy density becomes $\sim 5 \times 10^{-3} h^3$ Mpc$^{-3}$. For these assumed survey parameters, the non-Gaussian contribution to the covariance of the binned galaxy power spectrum is relatively minor and results in a relative increase, when compared with the Gaussian covariance, by a factor of 1.4 at $k \sim 0.25$ Mpc$^{-1}$, and by a factor of 2 at $k \sim 0.5$ Mpc$^{-1}$. Note that if the number density of galaxies were to be higher, such that the shot noise is reduced at small scales, then the relative importance of the non-Gaussian contribution to full covariance increases. The power spectrum is assumed to be that modelled from the halo approach with $\alpha = 0.8$ and $N_0 = 0.7$. We renormalized the power spectrum such that the bias factor is unity at large scales. We then model the galaxy power spectrum through a combination of the linear power spectrum and the constant bias, again assuming to be unity. The parameter errors and associated biases are tabulated in Table 1 for a $\Lambda$CDM cosmological model with a dark energy equation of state $w$ and allowing for massive neutrino contribution to the mass density of the Universe. We tabulated errors and biases as a function of the maximum $k$ value, $k_{\rm c}$, to which galaxy power spectrum analysis is considered to be linear. At typical large scales, with $k_{\rm c} = 0.1$ Mpc$^{-1}$, the biases are negligible and we recover parameter errors usually quoted in the literature by the Fisher matrix-based analyses similar to the one performed here (Eisenstein, Hu & Tegmark 1998; Wang, Spergel & Strauss 1999). In Table 1, we also tabulate errors expected from the galaxy power spectrum alone and the galaxy power spectrum combined with final *WMAP* data (middle rows) and with *Planck* data (bottom rows). The CMB information also includes polarization data in addition to temperature.

As one includes information out to smaller scales, or large $k_{\rm c}$ values, from the galaxy power spectrum, certain parameters, such as $\Omega_{\rm b}h^2$ and $m_\nu$, become better determined than out to an early cut-off, say at $k_{\rm c} = 0.1$ Mpc$^{-1}$. This can be understood by the fact that the small-scale regime of the galaxy power spectrum captures information related to these parameters through additional oscillatory features and the damping of power by massive neutrinos. This, however, comes at the expense of increasing biases in the parameter determination, since in this regime, non-linearities enter the galaxy power spectrum as the one-halo term becomes important and starts to dominate when $k > 0.6$ Mpc$^{-1}$ (see Fig. 1). Thus, the simple description based on the linear power spectrum and the scale-free bias breaks down when $k_{\rm c} > 0.1$ Mpc$^{-1}$ though there is a significant amount of cosmological information beyond this cut-off scale. Note that in Table 1 we do not consider $k_{\rm c}$ values above 0.5 since, for the survey parameters we have considered, the shot-noise term associated with the finite number density of galaxies starts to become important. For future surveys that attempt to measure an increased number of redshifts, it is clear that one gains further cosmological information by moving to smaller scales.

While cosmological parameter estimation from data below $\sim$0.1 Mpc$^{-1}$ is unaffected by non-linearities, it is useful to consider possibilities that can return information at wavenumbers above this value. This is due to the fact that current surveys, both 2dFGRS and SDSS,

as well as previous surveys, such as *IRAS* PCSZ, probed to much smaller scales than implied by this arbitrary cut-off. In the case of the real-space galaxy power spectrum, as shown in Fig. 1 (bottom panel), we consider the possibility that the onset of non-linearity can be modelled by a power-law contribution when wavenumbers out to 1 $\mathrm{Mpc}^{-1}$ are considered. In fact, for a good approximation, the one-halo term can be modelled as a power law in the mildly non-linear regime with

$$P_{1h}(k) = A_{nl} k^{\alpha_{nl}} \qquad \text{for } k < k_1. \tag{25}$$

This description includes three new parameters involving the normalization of the non-linear part of the power spectrum, $A_{nl}$, the slope, $\alpha_{nl}$, and the scale at which the power law breaks, $k_1$. Note that the power-law behaviour remains the same when one considers different models of the halo occupation number (Fig. 2).

The extent to which this approximation may be valid can be considered based on the halo model description of the non-linear galaxy power spectrum with the addition of a power-law contribution. While one can assume the halo model generated power spectrum as the expected non-linear power spectrum for galaxies, in parameter estimation, one can consider the model fitting procedure based on the approximation that the non-linear power spectrum is $P(k) = b^2(k)P^{lin}(k) + A_{nl}k^{\alpha_{nl}}$. The last two parameters account for the non-linearity and, more importantly, the power-law aspect of the one-halo term. Since at large scales $u_{gal}(k \mid m) \rightarrow 1$, one expects the normalization to be given by

$$A_{nl} = \int \mathrm{d}m\, n(m) \frac{\langle N_{gal}(N_{gal} - 1) \mid m \rangle}{\bar{n}_{gal}^2}, \tag{26}$$

and the power law $\alpha_{nl} \sim 0$ (in Fig. 1, $\alpha_{nl} \sim 3$ since we plot the logarithmic power spectrum, or $k^3\, P(k)/2\pi^2$). The departure from this expected power law captures the profile shape. Thus, if these two parameters can be extracted from the data as well, one obtains not only information related to cosmology, but also some aspect related to how galaxies populate dark matter haloes. The numerical value of $A_{nl}$, for example, can aid in constraining model-independent measurements of the halo occupation number (Cooray 2002b).

The extent to which this approximation may be valid is summarized in Fig. 5, for the same case as shown in Fig. 2. Here, we plot the ratio of the model power spectrum to that of the non-linear case as calculated by the halo model. As already discussed, the description that $P(k) = b^2(k)P^{lin}(k)$ breaks down rapidly such that at a wavenumber of 0.1 $\mathrm{Mpc}^{-1}$ one underestimates the true non-linear power by a few per cent, while at 0.3 $\mathrm{Mpc}^{-1}$ this underestimate is at the level of 25 per cent. Instead of $P(k) = b^2(k)P^{lin}(k)$, when one includes the additional power law such that $P(k) = b^2(k)P^{lin}(k) + A_{nl}k^{\alpha_{nl}}$, the difference is below a few per cent out to a wavenumber of 0.3 $\mathrm{Mpc}^{-1}$, suggesting that the transition is well modelled with the single power-law approximation. At a wavenumber of 0.5 $\mathrm{Mpc}^{-1}$, the power-law assumption leads to an overestimate of power at a level of 5 per cent, and this overestimate is at the level of 30 per cent when $k \sim 1$ $\mathrm{Mpc}^{-1}$, deep in the non-linear regime. While the single power-law assumption clearly breaks down at these small scales, the improvement over the simple linear assumption is significant when $k \sim 0.3$ $\mathrm{Mpc}^{-1}$.

While we have only considered a specific case with certain parameters for the halo occupation number in Fig. 5, we expect the situation to be the same with different descriptions. The extent to which one departs, however, is model-dependent, as we have shown in Fig. 2, especially with respect to the slope of the halo occupation number–halo mass relation (Fig. 2, top panel). The differences

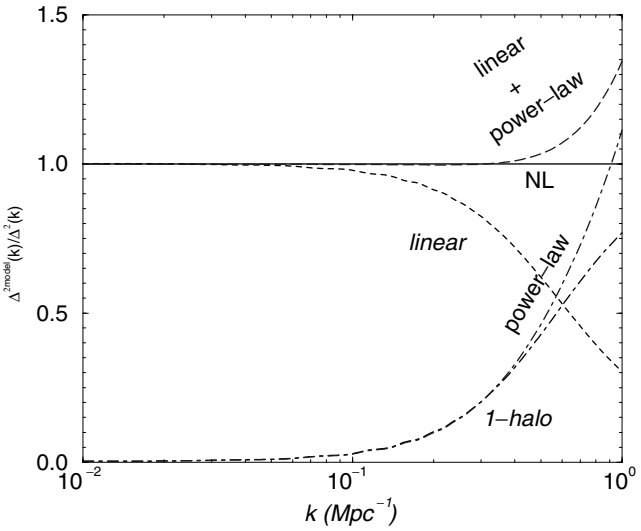


**Figure 5.** The ratio of modelled description of the galaxy power spectrum to that of the total power spectrum as expected under the halo model. The case illustrated here is the same as the one shown in Fig. 2. With the dotted line we show the linear power spectrum; as shown, the simple linear description with a constant bias leads to an underestimate of true power at the level of 20 per cent when $k \sim 0.2$–$0.3$ $\mathrm{Mpc}^{-1}$. This can be compensated with the addition of a power-law contribution. The ratio related to the linear plus a power law is shown with a long-dashed line. The agreement is essentially exact out to 0.3 $\mathrm{Mpc}^{-1}$, but results in an overestimate of power at deeply non-linear scales of 1 $\mathrm{Mpc}^{-1}$ and at the level of 30 per cent. For reference, with dot-dashed lines we show the one-halo contribution and the related power-law contribution that attempts to model the non-linear aspect related to the power spectrum.

move the non-linear scale from 0.05 to 0.2 $\mathrm{Mpc}^{-1}$, suggesting that the importance of the power law varies over the same scales for different samples of galaxies. The extent to which the power-law approximation works will similarly vary, and we note that, depending on $\alpha$, this can be between 0.3 and 0.5 $\mathrm{Mpc}^{-1}$, while departures are at the level of 10–50 per cent at 1 $\mathrm{Mpc}^{-1}$; if the power-law approximation is not included, the departures are substantial (>100 per cent). Regardless of the exact variations, such as on the extent to which the power-law assumption overestimates power when $k \sim 1$ $\mathrm{Mpc}^{-1}$, the power-law assumption provides a useful addition to the simple linear power spectrum description, with a constant bias, in mildly non-linear scales of order 0.2–0.4 $\mathrm{Mpc}^{-1}$.

Note that the power-law assumption is independent of selection effects and biases related to observational aspects. This can be understood simply as follows. The observed total power spectrum is simply a convolution of the real power spectrum times a window function that captures observational issues (equation 16). Since the true power spectrum can be described better with a combination of the linear power spectrum and a power-law correction, in the mildly non-linear scales, the observed power spectrum will remain essentially described by the same combination with the filtering aspects related to observations applied. Thus, regardless of how observations are done or how the galaxy power spectrum is measured, we expect our description to be accurate to the level where we can also describe the true underlying power spectrum with the same assumptions.

We can further understand the extent to which this model is valid by considering its ability to extract cosmological parameters. In Table 2, we list expected errors on cosmological parameters in addition to these two new astrophysically oriented parameters. While

**Table 2.** Marginalized errors with non-linearities accounted for by a power law.[a]

| | $k < 0.1$ Mpc$^{-1}$ | | | $k < 0.2$ Mpc$^{-1}$ | | | $k < 0.5$ Mpc$^{-1}$ | | |
|---|---|---|---|---|---|---|---|---|---|
| Parameter | Error | Bias | \|Bias\|/Error | Error | Bias | \|Bias\|/Error | Error | Bias | \|Bias\|/Error |
| $\ln(\Omega_b h^2)$ | 7.33 | 0.42 | 0.05 | 0.42 | 0.03 | 0.07 | 0.20 | 0.005 | 0.02 |
| $\ln(\Omega_m h^2)$ | 4.88 | 0.24 | 0.05 | 0.38 | 0.03 | 0.08 | 0.33 | 0.02 | 0.06 |
| $m_\nu$ (eV) $\propto \Omega_\nu h^2$ | 7.27 | −0.14 | 0.02 | 1.74 | −0.10 | 0.06 | 1.50 | −0.04 | 0.03 |
| $\Omega_\Lambda$ | $\infty$ | – | – | $\infty$ | – | – | $\infty$ | – | – |
| $w$ | $\infty$ | – | – | $\infty$ | – | – | $\infty$ | – | – |
| $n_S(k_{\rm fid})$ | 0.78 | −0.02 | 0.03 | 0.12 | −0.01 | 0.08 | 0.11 | −0.01 | 0.09 |
| $\ln P_\Phi(k_{\rm fid}) \equiv \ln A_S^2$ | $\infty$ | – | – | 2.36 | −0.11 | 0.06 | 0.94 | 0.09 | 0.09 |
| $\ln b$ | $\infty$ | – | – | 1.64 | 0.11 | 0.06 | 0.82 | 0.07 | 0.08 |
| $A_{\rm nl}$ | $\infty$ | – | – | 3.95 | 0.31 | 0.08 | 0.41 | 0.06 | 0.14 |
| $\alpha_{\rm nl}$ | $\infty$ | – | – | 3.58 | −0.14 | 0.04 | 0.45 | −0.05 | 0.11 |
| $\ln(\Omega_b h^2)$ | 0.25 | 0.00 | 0.02 | 0.024 | 0.00 | 0.05 | 0.02 | 0.00 | 0.05 |
| $\ln(\Omega_m h^2)$ | 0.06 | 0.00 | 0.04 | 0.05 | 0.00 | 0.02 | 0.05 | 0.00 | 0.04 |
| $m_\nu$ (eV) $\propto \Omega_\nu h^2$ | 0.41 | −0.03 | 0.07 | 0.25 | −0.01 | 0.04 | 0.23 | −0.01 | 0.04 |
| $\Omega_\Lambda$ | 0.06 | 0.00 | 0.01 | 0.06 | 0.00 | 0.02 | 0.06 | 0.00 | 0.02 |
| $w$ | 0.30 | 0.01 | 0.04 | 0.28 | 0.02 | 0.06 | 0.27 | 0.00 | 0.02 |
| $n_S(k_{\rm fid})$ | 0.019 | 0.00 | 0.04 | 0.016 | −0.00 | 0.07 | 0.01 | −0.00 | 0.01 |
| $\ln P_\Phi(k_{\rm fid}) \equiv \ln A_S^2$ | 0.020 | 0.00 | 0.03 | 0.018 | 0.00 | 0.08 | 0.016 | 0.00 | 0.05 |
| $\ln b$ | 0.13 | 0.00 | 0.06 | 0.036 | 0.00 | 0.03 | 0.034 | 0.00 | 0.06 |
| $A_{\rm nl}$ | $\infty$ | – | – | 2.27 | 0.21 | 0.09 | 0.22 | 0.04 | 0.18 |
| $\alpha_{\rm nl}$ | $\infty$ | – | – | 1.98 | −0.12 | 0.06 | 0.23 | 0.03 | 0.13 |
| $\ln(\Omega_b h^2)$ | 0.005 | 0.00 | 0.00 | 0.006 | 0.00 | 0.01 | 0.005 | 0.00 | 0.04 |
| $\ln(\Omega_m h^2)$ | 0.015 | 0.00 | 0.02 | 0.014 | 0.00 | 0.02 | 0.014 | 0.00 | 0.07 |
| $m_\nu$ (eV) $\propto \Omega_\nu h^2$ | 0.18 | −0.00 | 0.02 | 0.14 | −0.00 | 0.01 | 0.10 | −0.00 | 0.01 |
| $\Omega_\Lambda$ | 0.05 | 0.00 | 0.00 | 0.05 | 0.00 | 0.00 | 0.05 | 0.00 | 0.00 |
| $w$ | 0.17 | 0.00 | 0.01 | 0.17 | 0.00 | 0.01 | 0.17 | 0.01 | 0.05 |
| $n_S(k_{\rm fid})$ | 0.004 | −0.00 | 0.01 | 0.004 | −0.00 | 0.01 | 0.003 | −0.00 | 0.01 |
| $\ln P_\Phi(k_{\rm fid}) \equiv \ln A_S^2$ | 0.005 | −0.00 | 0.01 | 0.005 | 0.00 | 0.02 | 0.004 | 0.00 | 0.02 |
| $\ln b$ | 0.12 | 0.01 | 0.08 | 0.025 | 0.00 | 0.08 | 0.016 | 0.00 | 0.06 |
| $A_{\rm nl}$ | $\infty$ | – | – | 1.76 | 0.18 | 0.10 | 0.18 | 0.02 | 0.11 |
| $\alpha_{\rm nl}$ | $\infty$ | – | – | 1.51 | −0.11 | 0.07 | 0.19 | 0.02 | 0.10 |

[a]Same as Table 1. We add two extra parameters: the normalization of the non-linear contribution to the galaxy power spectrum, $A_{\rm nl}$, and its power-law slope, $\alpha_{\rm nl}$, with scale. In the case of our fiducial model and a logarithmic power spectrum, the two parameters have numerical values of 65.7 and 3.04, respectively. Note the reduction in parameter biases compared with Table 1.

cosmological parameter estimates either remain the same as in Table 1 or worsen slightly, we note there is a sharp reduction in biases associated with parameter measurements when power spectrum information out to wavenumbers of 0.5 Mpc$^{-1}$ is included. This is significant since the assumed power-law behaviour around the onset of non-linearity allows one to measure cosmology from previously ignored non-linear scales such that no biases are introduced. In Fig. 6, as an example, we show the measurement errors for two parameters ($\Omega_m h^2$ and $m_\nu$) by marginalizing over all other parameters. We show expected errors in combination with *WMAP* and *Planck* and the improvement when information out to 0.5 Mpc$^{-1}$ is included with two additional parameters to be determined from data. Including information out to 0.5 Mpc$^{-1}$ improves parameter errors; for example, in the case of neutrino mass, by roughly a factor of 2.

So far, we have only considered the real-space galaxy power spectrum. A similar situation exists for the redshift-space power spectrum, though, as discussed in Section 2.2, the onset of its non-linearity is associated with a decrease in power, relative to linear power spectrum times a constant bias, instead of an increase. To model this behaviour, one can introduce an additional damping term associated with non-linear pairwise velocity to the usual formula involving the linear power spectrum (Ballinger, Heavens & Taylor 1996; Hatton & Cole 1998; Kang et al. 2002). This leads to a modification to equation (9):

$$\delta_{\rm g}^z(\boldsymbol{k}) = \delta_{\rm g}(\boldsymbol{k}) \frac{(1+\beta\mu^2)}{(1+k^2\mu^2\sigma^2/2)^{1/2}}, \tag{27}$$

such that the angular averaged redshift-space power spectrum takes the form of

$$P_{z,{\rm gal}}(k) = \left\{ \frac{(\beta^2 k^2\sigma^2 - 6\beta^2 + 6\beta k^2\sigma^2)}{6(k^2\sigma^2/2)^2} + \frac{(\beta - k^2\sigma^2/2)^2 \arctan(\sqrt{k^2\sigma^2/2})}{(k^2\sigma^2/2)^{5/2}} \right\} b_{\rm g}^2 P^{\rm lin}(k), \tag{28}$$

where $\beta = f(\Omega_m)/b_g$, as before, and $b_g$ is the scale-free large-scale galaxy bias. When $\sigma \to 0$, this formula is equivalent to the standard formula used in cosmological interpretations with the linear power spectrum scaled by the factor $(1 + \frac{2}{3}\beta + \frac{1}{5}\beta^2)b_g^2$. Note that such a correction only accounts for the increase in power at large scale associated with bulk motions. At small scales, with wavenumbers $\sim$0.1 Mpc$^{-1}$ and larger, it is necessary to account for suppression of power related to virial motions with dispersion $\sigma$, and we suggest the use of equation (28). In order to account for the one-halo part of the non-linear redshift-space power spectrum, especially for an

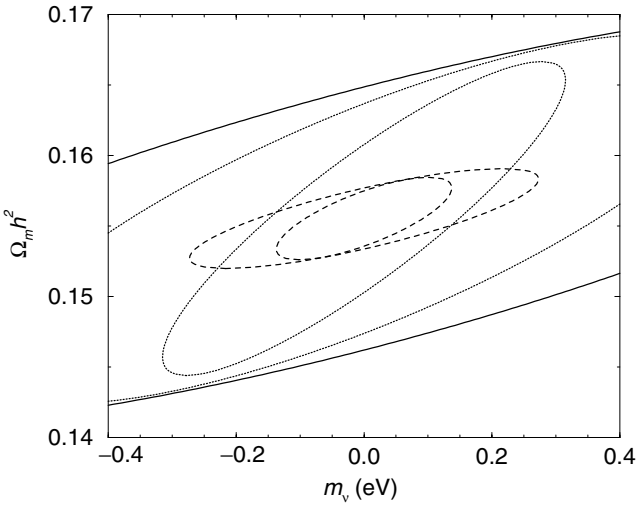


**Figure 6.** The $1\sigma$ error ellipses for determination of $\Omega_{\rm m}h^2$ and the neutrino mass. These errors follow from Tables 1 and 2. The solid line shows the constraint expected from the three-year *WMAP* data set (including polarization information). The dotted lines show the expected improvement when galaxy clustering information is added with a cut-off at $k < 0.1\,{\rm Mpc}^{-1}$ and using information out to $0.5\,{\rm Mpc}^{-1}$ with account taken of non-linearities (see text). The dashed lines show the same situation but with *Planck* as the source of information related to CMB. The galaxy clustering survey considered here is equivalent to that of the SDSS.

analysis of data beyond a wavenumber of $\sim$1 Mpc$^{-1}$, one can introduce again a power law, following the suggested approach for the non-linear real-space power spectrum. At mildly non-linear scales, the approach suggested here leads to an additional parameter, $\sigma$, which can be simultaneously determined from data in addition to cosmological estimates. Currently, the well-studied redshift-space power spectrum comes from the 2dF survey, and we plan to return to these issues as part of a combined modelling effort on non-linearities in this power spectrum based on cosmology as well as simplified corrections based on the halo approach.

## 4 SUMMARY

The galaxy power spectrum is now a well-known tool of precision cosmology. Ongoing surveys such as 2dF and SDSS have already provided a wealth of information related to cosmological parameters based on clustering of galaxies in the presumed linear regime, though measurements span down to much smaller scales than used for cosmological purposes. We have shown here that there is a considerable amount on information in the regime where clustering transits from linear to non-linear. The extraction of this information, however, cannot be done alone with the usual approach involving the linear power spectrum and a constant scale-free bias. We have investigated the non-linear behaviour of the galaxy power spectrum in both real and redshift space based on the halo approach and have suggested that the onset of non-linearities can be modelled as a simple power law. The normalization and the power-law slope provide certain information related to halo occupation description in the halo models of galaxy clustering. We have shown that significant improvements can be made when non-linear effects are taken into account through this power-law contribution with two additional parameters to be determined from the data simultaneously with cosmological parameters. The suggested approach can easily be implemented in current cosmological studies of galaxy clustering and to extract most information from galaxy clustering data to date.

## ACKNOWLEDGMENTS

We acknowledge useful discussions with O. Lahav on the 2dFGRS power spectrum. This work is supported by the Sherman Fairchild foundation and DOE DE-FG 03-92-ER40701. AC thanks the Kvali Institute for Theoretical Physics (supported by NSF PHY99-07949) for hospitality where this work was initiated.

## REFERENCES

Ballinger W. E., Heavens A. F., Taylor A. N., 1995, MNRAS, 276, 59
Bartelmann M., Schneider P., 2001, Phys. Rep., 340, 291
Benson A. J., Cole S., Frenk C. S., Baugh C. M., Lacey C. G., 2000, MNRAS, 311, 793
Berlind A. A., Weinberg D. H., 2002, ApJ, 575, 587
Berlind A. A. et al., 2003, ApJ, 593, 1
Blake C., Glazebrook K., 2003, ApJ, 594, 665
Colless M. et al., 2001, MNRAS, 328, 1039
Cooray A., 2002a, in Klapdor-Kleingrothaus H., Viollier R., eds, Dark 2002: Dark Matter in Astro- and Particle-Physics. Springer, Berlin (astro-ph/0204090)
Cooray A., 2002b, ApJ, 576, L105
Cooray A., Hu W., 2001, ApJ, 554, 56
Cooray A., Sheth R., 2002, Phys. Rep., 372, 1
Cooray A., Hu W., Huterer D., Joffre M., 2001, ApJ, 557, L75
Eisenstein D. J., 2002, in Brown M., Dey A., eds, ASP Conf. Ser. Vol. 280, Next Generation Wide-Field Multi-Object Spectroscopy. Astron. Soc. Pac., San Francisco (astro-ph/0301623)
Eisenstein D. J., Hu W., 1998, ApJ, 496, 605
Eisenstein D. J., Hu W., Tegmark M., 1998, ApJ, 518, 2
Elgaroy O., Lahav O., 2003, J. Cosmol. Astropart. Phys., 04, 4
Elgaroy O., Gramann M., Lahav, O., 2002, MNRAS, 333, 93
Haiman Z., Mohr J. J., Holder G. P., 2001, ApJ, 553, 545
Hamilton A. J. S., Tegmark M., 2002, MNRAS, 330, 506
Hatton S. J., Cole S., 1998, MNRAS, 296, 10
Holder G. P. et al., 2000, ApJ, 544, 629
Huterer D., 2002, Phys. Rev. D, 65, 063001
Kaiser N., 1987, MNRAS, 227, 1
Kang X., Jing Y. P., Mo H. J., Borner G., 2002, MNRAS, 336, 892
Kauffmann G., Colberg J. M., Diaferio A., White S. D. M., 1999, MNRAS, 303, 188
Kendall M. G., Stuart A., 1969, The Advanced Theory of Statistics, Vol. II. Griffin, London
Magliocchetti M., Porciani C., 2003, MNRAS, 346, 186
Massey R. et al., 2003, preprint (astro-ph/0304418)
Meiksin A., White M., 1999, MNRAS, 308, 1179
Meiksin A., White M., Peacock J. A., 1996, MNRAS, 304, 851
Miller C. J., Nichol R. C., Batuski D. J., 2001, Sci, 292, 2302
Mo H. J., White S. D. M., 1996, MNRAS, 282, 347
Navarro J., Frenk C., White S. D. M., 1996, ApJ, 462, 563
Outram P. J., Hoyle F., Shanks T., Boyle B. J., Croom S. M., Loaring N. S., Miller L., Smith R. J., 2001, MNRAS, 328, 174
Peacock J. A., West M. J., 1992, MNRAS, 259, 494
Peacock J. A., Smith, R. E., 2000, MNRAS, 318, 1144
Peacock J. A. et al., 2001, Nat, 410, 169
Percival W. J. et al., 2001, MNRAS, 327, 1297
Percival W. J. et al., 2002, MNRAS, 335, 432
Press W. H., Schechter P., 1974, ApJ, 187, 425
Saunders W. et al., 1990, MNRAS, 242, 318
Scoccimarro R., Zaldarriaga M., Hui L., 1999, ApJ, 527, 1
Scoccimarro R., Sheth R., Hui L., Jain B., 2001, ApJ, 546, 20
Seljak U., 2000, MNRAS, 318, 203
Seljak U., 2001, MNRAS, 325, 1359

Sheth R. K., Diaferio A., 2001, MNRAS, 322, 901
Stark A. A. et al., 1998, preprint (astro-ph/9802326)
Strauss M. A., Willick J. A., 1995, Phys. Rep., 261, 271
Sunyaev R. A., Zel'dovich Ya. B., 1980, MNRAS, 190, 413
Tegmark M., Taylor A., Heavens A., 1997, ApJ, 480, 22
Tyson J. A., Wittman D., Angel J. R. P., 2000, in Cline D. B., ed., The dark matter telescope, Dark Matter 2000. Elsevier, Amsterdam (astro-ph/0005381)
Wang Y., Spergel D. N., Strauss M. A., 1999, ApJ, 510, 20
Wittman D., Tyson J. A., Margoniner V. E., Cohen J. G., Dell'Antonio I. P., 2001, ApJ, 557, L89
York D. G. et al., 2000, AJ, 120, 1579

This paper has been typeset from a TEX/LATEX file prepared by the author.